Memory effects on descent from nuclear fission barrier

V.M. Kolomietz[1,2)], S.V. Radionov[1)] and S. Shlomo[2)]
[1)] *Institute for Nuclear Research, Kiev 03028, Ukraine*
[2)] *Cyclotron Institute, Texas A&M University, College Station, Texas 77843, USA*

Abstract

Non-Markovian transport equations for nuclear large amplitude motion are derived from the collisional kinetic equation. The memory effects are caused by the Fermi surface distortions and depend on the relaxation time. It is shown that the nuclear collective motion and the nuclear fission are influenced strongly by the memory effects at the relaxation time $\tau \geq 5 \cdot 10^{-23}$s. In particular, the descent of the nucleus from the fission barrier is accompanied by characteristic shape oscillations. The eigenfrequency and the damping of the shape oscillations depend on the contribution of the memory integral in the equations of motion. The shape oscillations disappear at the short relaxation time regime at $\tau \to 0$, which corresponds to the usual Markovian motion in the presence of friction forces. We show that the elastic forces produced by the memory integral lead to a significant delay for the descent of the nucleus from the barrier. Numerical calculations for the nucleus ^{236}U shows that due to the memory effect the saddle-to-scission time grows by a factor of about 3 with respect to the corresponding saddle-to-scission time obtained in liquid drop model calculations with friction forces.

PACS number: 21.60.Ev, 25.85.Ca

I. INTRODUCTION

The dynamics of a nucleus undergoing fission can be studied in terms of only a few collective variables like nuclear shape parameters [1]. Such kind of approach is usually associated with the liquid drop model (LDM) and its extensions and is acceptable for a slow collective motion where the fast intrinsic degrees of freedom exert forces on the collective variables leading to a Markovian transport equation. An essential assumption is that the LDM provides a good approximation for a smooth part, $\widetilde{E}_{\rm pot}$, of the collective potential energy, $E_{\rm pot}$, and can be then used for the quantum calculations of $E_{\rm pot}$ within Strutinsky's shell correction method [2], obtaining $E_{\rm pot} = \widetilde{E}_{\rm pot} + \delta\mathcal{U}$, where $\delta\mathcal{U}$ is the shell correction. On the other hand, it is well known that the LDM is not able to describe some strongly collective nuclear excitations such as the isoscalar giant multipole resonances. It is because the LDM ignores the important features of the nucleus as a Fermi liquid. The collective motion of the nuclear Fermi liquid is accompanied by the dynamical distortion of the Fermi-surface [3] and the smooth energy $\widetilde{E}_{\rm pot}$ is subsidized by an additional contribution, $\widetilde{E}_{\rm pot,F}$, which is caused by the *dynamic* Fermi-surface distortion effect and is absent in the standard LDM [4,5]. We point out that the energy $\widetilde{E}_{\rm pot,F}$ is a smooth quantity (in the sense of the shell correction method) and it can not be recovered by taking into consideration the quantum shell corrections to the adiabatic (static) potential energy deformation. This situation becomes more clear in the limit of the infinite Fermi system with $A \to \infty$, where A is the number of particles. The shell correction $\delta\mathcal{U}$ disappears at $A \to \infty$. In this case, the adiabatic collective energy $E_{\rm pot} = \widetilde{E}_{\rm pot}$, caused by a change of the particle density ρ with respect to its equilibrium value $\rho_{\rm eq}$, determines the first sound velocity $c_1 = \sqrt{K/9m}$, where K is the incompressibility coefficient given by

$$K = \frac{\partial^2(E_{\rm pot}/A)}{\partial\rho^2}\rho^2|_{\rm eq} \approx \frac{\partial^2(\widetilde{E}_{\rm pot}/A)}{\partial\rho^2}\rho^2|_{\rm eq}.$$

However, it is well known [6,7] that, in a cold Fermi liquid, the first sound velocity c_1 is relevant only in the limit of strong interaction, i.e., at $|F_0| \gg 1$, where F_0 is the Landau parameter in the quasiparticle scattering amplitude. For the normal nuclear matter we have rather the value of $F_0 \sim 0$, which can be derived from the Skyrme forces [8]. The corresponding sound velocity (zero sound velocity) c_0 exceeds the velocity c_1 by a factor of about $\sqrt{3}$ at $F_0 \sim 0$ [7]. This difficulty is overcome if the additional contribution $\widetilde{E}_{\rm pot,F}$ to the potential energy $\widetilde{E}_{\rm pot}$ is taken into account [9]. Thus, the smooth energy $\widetilde{E}_{\rm pot,F}$, caused by the Fermi surface distortion effect, is a necessary ingredient of the dynamics of the nuclear Fermi liquid. It is absent in the adiabatic deformation energy $\widetilde{E}_{\rm pot}$ derived by the traditional LDM.

The equations of motion for the nuclear Fermi liquid can be derived from the collisional kinetic equation [3]. In general, the corresponding equations of motion are non-Markovian [10,11]. The memory effects appear here due to the Fermi-surface distortion and depend on the relaxation time [12,13]. The Markovian dynamic is achieved in two limiting cases only: (i) short relaxation time limit which corresponds to the first sound propagation in infinite Fermi liquid. In fact, this limit is realized by the nuclear LDM, (ii) infinite relaxation time limit which corresponds to the zero sound propagation with a strong renormalization of the

sound velocity and the deformation energy with respect to the ones in the LDM. The non-Markovian-Langevin equations of motion for macroscopic collective variables were earlier derived in [14] and used for the small amplitude dynamics [5,15] and for some aspects of the induced nuclear fission and the fission rate problem [16].

The main purpose of the present paper is to apply the non-Markovian dynamics to the descent of the nucleus from the fission barrier. Starting from the collisional Landau-Vlasov kinetic equation, we suggest a new proof of the non-Markovian equations of motion for the nuclear shape variables which establishes a direct connection between the memory effects and with the dynamic distortion of the Fermi surface. In contrast to Ref. [16], we do not take into consideration the random forces and only concentrate on the formation of both the conservative and the friction forces behind the saddle point to clarify the effects of the memory integral. In this aspect, our approach represents an extension of the traditional LDM theory of the nuclear fission [1,17–19] to the case of the Fermi liquid and takes into account the important features of the dynamic Fermi surface distortion which are ignored in the LDM.

The plan of the paper is as follows. In Sec. II we obtain the Euler-like equation of motion for the displacement field. This equation contains the memory dependent pressure tensor. Assuming that the nucleus is an incompressible and irrotational fluid and using the boundary conditions for the velocity field, we reduce the local Euler-like equation to the non-Markovian equations of motion for the shape variables. The transport coefficients and the memory kernel are derived through the solution to the Neumann problem for the potential of the velocity field. In Sec. III we study the dependence of the memory effects on the relaxation time for both the small amplitude motion near the saddle point and for the descent of the nucleus from the barrier to the scission point. Summary and conclusions are given in Sec. IV.

II. NON-MARKOVIAN DYNAMICS OF NUCLEAR FERMI LIQUID DROP

To derive the equation of motion for the shape variables, we will start from the collisional kinetic equation for the phase-space distribution function $f \equiv f(\mathbf{r}, \mathbf{p};t)$ in the following general form

$$\frac{\partial}{\partial t} f + \frac{\mathbf{p}}{m} \cdot \nabla_r f - \nabla_r U \cdot \nabla_p f = I[f], \tag{1}$$

where $U \equiv U(\mathbf{r}, \mathbf{p};t)$ is the selfconsistent mean field and $I[f]$ is the collision integral. The momentum distribution is distorted during the time evolution of the system and the distribution function takes the form

$$f(\mathbf{r}, \mathbf{p};t) = f_{\rm sph}(\mathbf{r}, \mathbf{p};t) + \sum_{l \geq 1} \delta f_l(\mathbf{r}, \mathbf{p};t), \tag{2}$$

where $f_{\rm sph}(\mathbf{r}, \mathbf{p};t)$ describes the spherical distribution in momentum space and l is the multipolarity of the Fermi-surface distortion. We point out that the time dependent Thomas-Fermi (TDTF) approximation and the corresponding nuclear LDM are obtained from Eq. (1) if one takes the distribution function $f(\mathbf{r}, \mathbf{p};t)$ in the following restricted form

$f_{\rm TF}(\mathbf{r},\mathbf{p};t) = f_{\rm sph}(\mathbf{r},\mathbf{p};t) + \delta f_{l=1}(\mathbf{r},\mathbf{p};t)$ instead of Eq. (2), see Ref. [20]. Below we will extend the TDTF approximation taking into account the dynamic Fermi surface distortion up to multipolarity $l = 2$ [4,5,21]. We will also assume that the collective motion is accompanied by a small deviation of the momentum distribution from the spherical symmetry, i.e., even in the case of large amplitude motion the main contribution to the distribution function $f(\mathbf{r},\mathbf{p};t)$ is given the Thomas-Fermi term $f_{\rm TF}(\mathbf{r},\mathbf{p};t)$ and the additional term $\delta f_{l=2}(\mathbf{r},\mathbf{p};t)$ provides only small corrections. The lowest orders $l = 0$ and 1 (which are not necessary small) of the Fermi-surface distortion do not contribute to the collision integral because of the conservation laws [3] and the linearized collision integral with respect to small perturbation $\delta f_{l=2}(\mathbf{r},\mathbf{p};t)$, is given by

$$I[f] = -\frac{\delta f_{l=2}}{\tau}, \tag{3}$$

where τ is the relaxation time.

Evaluating the first three moments of Eq. (1) in $\mathbf{p}$-space, we can derive a closed set of equations for the following moments of the distribution function, namely, local particle density ρ, velocity field u_ν and pressure tensor $P_{\nu\mu}$, in the form (for details, see Refs. [20,22])

$$\frac{\partial}{\partial t}\rho = -\nabla_\nu(\rho u_\nu), \tag{4}$$

$$m\rho\frac{\partial}{\partial t}u_\nu + m\rho\ (u_\mu\nabla_\mu)\ u_\nu + \nabla_\nu\mathcal{P} + \rho\nabla_\nu\frac{\delta\epsilon_{\rm pot}}{\delta\rho} = -\nabla_\mu P'_{\nu\mu}, \tag{5}$$

$$\frac{\partial}{\partial t}P'_{\nu\mu} + \mathcal{P}\ \frac{\partial}{\partial t}\Lambda_{\nu\mu} = -\frac{1}{\tau}P'_{\nu\mu}, \tag{6}$$

where $\mathcal{P} \equiv \mathcal{P}(\mathbf{r},t)$ is the isotropic part of the pressure tensor

$$\mathcal{P}(\mathbf{r},t) = \frac{1}{3m}\int\frac{d\mathbf{p}}{(2\pi\hbar)^3}p^2 f_{\rm sph}(\mathbf{r},\mathbf{p};t), \tag{7}$$

$P'_{\nu\mu} = P'_{\nu\mu}(\mathbf{r},t)$ is the deviation of the pressure tensor from its isotropic part, $\mathcal{P}(\mathbf{r},t)$, due to the Fermi surface distortion

$$P'_{\nu\mu}(\mathbf{r},t) = \frac{1}{m}\int\frac{d\mathbf{p}}{(2\pi\hbar)^3}(p_\nu - mu_\nu)(p_\mu - mu_\mu)\delta f_{l=2}(\mathbf{r},\mathbf{p};t), \tag{8}$$

$\epsilon_{\rm pot}$ is the potential energy density related to the selfconsistent mean field U as $U = \delta\epsilon_{\rm pot}/\delta\rho$. The tensor $\Lambda_{\nu\mu}$ in Eq. (6) is given by

$$\Lambda_{\nu\mu} = \nabla_\nu\chi_\mu + \nabla_\mu\chi_\nu - \frac{2}{3}\delta_{\nu\mu}\nabla_\lambda\chi_\lambda, \tag{9}$$

where $\chi_\nu \equiv \chi_\nu(\mathbf{r},t)$ is the displacement field related to the velocity field as $u_\nu \equiv u_\nu(\mathbf{r},t) = \partial\chi_\nu(\mathbf{r},t)/\partial t$. From Eq. (6) we find the pressure tensor $P'_{\nu\mu}(\mathbf{r},t)$ in the following form

$$P'_{\nu\mu}(\mathbf{r},t) = P'_{\nu\mu}(\mathbf{r},t_0) - \int_{t_0}^{t}dt'\exp(\frac{t'-t}{\tau})\ \mathcal{P}(\mathbf{r},t')\ \frac{\partial}{\partial t'}\Lambda_{\nu\mu}(\mathbf{r},t'). \tag{10}$$

The tensor $P'_{\nu\mu}(\mathbf{r},t_0)$ is determined by the initial conditions. In the case of the quadrupole distortion of the Fermi surface, the tensor $P'_{\nu\mu}(\mathbf{r},t_0)$ is derived by the initial displacement field χ_ν.

Assuming that the nucleus is an incompressible and irrotational fluid with a sharp surface in $\mathbf{r}$-space, we will reduce the local equation of motion (5) to the equations for the variables $q = \{q_1, q_2, ...q_N\}$ that specify the shape of the nucleus. The continuity equation (4) has to be complemented by the boundary condition on the moving nuclear surface S. Below we will assume that the axially symmetric shape of the nucleus is defined by rotation of the profile function $\rho = Y(z, \{q_i(t)\})$ around the z-axis in the cylindrical co-ordinates ρ, z, φ [24,25]. The velocity of the nuclear surface is then given by [25]

$$u_S = \sum_{i=1}^{N} \bar{u}_i \dot{q}_i, \tag{11}$$

where

$$\bar{u}_i = (\partial Y/\partial q_i)/\Lambda, \quad \Lambda = \sqrt{1 + (\partial Y/\partial z)^2}. \tag{12}$$

The potential of the velocity field takes the form

$$\phi = \sum_{i=1}^{N} {}_i\overline{\phi}\ \dot{q}_i, \tag{13}$$

where the potential field $\overline{\phi}_i \equiv \overline{\phi}_i(\mathbf{r},q)$ is determined by the equations of the following Neumann problem [25]

$$\nabla^2\ \bar{\phi}_i = 0\,, \qquad (\mathbf{n}\nabla\ \bar{\phi}_i)_S = \frac{1}{\Lambda}\frac{\partial Y}{\partial q_i}, \tag{14}$$

where $\mathbf{n}$ is the unit vector which is normal to the nuclear surface.

Using Eqs. (5) and (10) with $u_\nu = \nabla_\nu\phi$, multiplying Eq. (5) by $\nabla_\mu\overline{\phi}_i$ and integrating over $\mathbf{r}$, one obtains

$$\sum_{j=1}^{N}[B_{ij}(q)\ddot{q}_j + \sum_{k=1}^{N}\frac{\partial B_{ij}}{\partial q_k}\ \ \dot{q}_j\dot{q}_k + \int_{t_0}^{t} dt' \exp(\frac{t'-t}{\tau})\kappa_{ij}(t,t')\ \ \dot{q}_j\ (t')] = -\frac{\partial E_{\rm pot}(q)}{\partial q_i}. \tag{15}$$

Here $B_{ij}(q)$ is the inertia tensor

$$B_{ij}(q) = m\rho_0 \oint ds\bar{u}_i\ \overline{\phi}_j, \tag{16}$$

where ρ_0 is the nuclear bulk density. The adiabatic collective potential energy, $E_{\rm pot}(q)$, does not contain the contribution from the Fermi-surface distortion effect and is given by

$$E_{\rm pot}(q) = \int d\mathbf{r}\ (\epsilon_{\rm kin}(\mathbf{r},q) + \epsilon_{\rm pot}(\mathbf{r},q)), \tag{17}$$

where $\epsilon_{\rm kin}(\mathbf{r},q)$ is the kinetic energy of the internal motion of nucleons. The memory kernel $\kappa_{i,j}(t,t')$ in Eq. (15) is given by

$$\kappa_{ij}(t,t') = 2 \int d\mathbf{r}\ \mathcal{P}(\mathbf{r},q(t'))\ (\nabla_\nu \nabla_\mu\ \bar{\phi}_i\ (\mathbf{r},q(t)))\ (\nabla_\nu \nabla_\mu\ \bar{\phi}_j\ (\mathbf{r},q(t'))). \tag{18}$$

In Eq. (15), we have omitted the contribution from the initial distortion of the Fermi surface caused by the pressure tensor $P'_{\nu\mu}(\mathbf{r},t_0)$. The contribution from $P'_{\nu\mu}(\mathbf{r},t_0)$ reflects the fact that the initial displacement field $\chi_\mu(\mathbf{r},t_0)$ is switched on suddenly at $t = t_0$. The adiabatic force $-\partial E_{\rm pot}(q)/\partial q$ in Eq. (15) obtains then the additional contribution at $t = t_0$ due to the initial distortion of the Fermi surface. However the corresponding force is absent if the initial displacement field $\chi_\mu(\mathbf{r},t_0)$ is obtained as a result of the previous evolution of the system at $t < t_0$. Below we will consider the descent of the nucleus from the fission barrier, i.e. assume the presence of the evolution of the system at $t < t_0$, and omit the contribution from the pressure tensor $P'_{\nu\mu}(\mathbf{r},t_0)$.

The displacement field $\chi_\nu(\mathbf{r},q)$ and the potential field $\overline{\phi}_i \equiv \overline{\phi}_i(\mathbf{r},q)$ are determined by a solution to the Neumann problem (14). The displacement field $\chi_\nu(\mathbf{r},q)$ can be also obtained using the Werner-Wheeler method [24]. In the cylindrical co-ordinates ρ, z, φ, the components of velocity field u_z and u_ρ in z and ρ directions are then approximated as [24]

$$u_z = \sum_i \mathcal{A}_i(z,q)\dot{q}_i \quad , \quad u_\rho = \frac{\rho}{Y(z,q)} \sum_i \mathcal{B}_i(z,q)\dot{q}_i. \tag{19}$$

The two unknown coefficients $\mathcal{A}_i(z,q)$ and $\mathcal{B}_i(z,q)$ are related to each other by means of continuity equation as

$$\mathcal{B}_i(z,q) = -\frac{1}{2} Y(z,q) \frac{\partial \mathcal{A}_i(z,q)}{\partial z}. \tag{20}$$

Requiring then that the normal velocity of the fluid on the surface should coincide with the normal velocity of the surface one can express the coefficient $\mathcal{A}_i(z,q)$ in terms of the profile function $Y(z,q)$ as

$$\mathcal{A}_i(z,q) = Y^{-2}(z,q) \frac{\partial}{\partial q_i} \int_z^{z_{\rm max}} dz' Y^2(z',q). \tag{21}$$

We point out that in the case of irrotational flow the Werner-Wheeler method leads to a velocity field potential of quadrupole type [25]

$$\phi(\mathbf{r},q) = \frac{1}{4q}\ (2\ z^2 - x^2 - y^2). \tag{22}$$

A spheroidal figure presents the simplest example which is consistent with the velocity field potential (22). In this case $q = q(t)$ is the elongation of the figure in units of the radius $R_0 = r_0 A^{1/3}$ of the nucleus and the equation of motion (15) takes the following form

$$B(q)\ \ddot{q} + \frac{\partial B(q)}{\partial q}\ \dot{q}^2 = -\frac{\partial E_{\rm pot}(q)}{\partial q} - \int_{t_0}^{t} dt' \exp(\frac{t'-t}{\tau}) \kappa(t,t')\ \ \dot{q}\ (t'). \tag{23}$$

Here, the mass parameter $B(q)$ and the memory kernel $\kappa(t,t')$ are given by

$$B(q) = \frac{1}{5}\ A\ m\ R_0^2\ \left(1 + \frac{1}{2q^3}\right) \quad \text{and} \quad \kappa(t,t') = \frac{\kappa_0}{q(t)\ q(t')}, \tag{24}$$

where $\kappa_0 = (4/5\ m)\ \pi\ \rho_0\ p_F^2\ R_0^3$ and p_F is the Fermi momentum.

III. NUMERICAL CALCULATIONS AND DISCUSSION

Let us start from the one-dimension case and apply Eq. (23) to the large amplitude motion from the barrier point B to the "scission" point C in Fig. 1. Following the Kramers model [26], we will approximate the potential energy $E_{\rm pot}(q)$ by an upright oscillator $(1/2)C_{LDM}(q-q_0)^2$ with $q_0=1$ and an inverted oscillator $E_f-(1/2)\widetilde{C}_{LDM}(q-q_f)^2$ which are joined smoothly as shown in Fig. 1 (see also Ref. [27]). Let us consider, first of all, a small amplitude change, Δq, of the shape variable, q, near both the ground state at $q\sim q_0=1$ with $\Delta q=q-q_0$ and at the saddle point at $q\sim q_f$ with $\Delta q=q-q_f$. Linearizing Eq. (23), we will rewrite it as

$$\widetilde{B}\ \frac{\partial^2}{\partial t^2}\Delta q\ =-\ k\ \Delta q-\widetilde{\kappa}\int_{t_0}^{t}dt'\exp(\frac{t'-t}{\tau})\ \frac{\partial}{\partial t'}\Delta q(t'), \tag{25}$$

where $\widetilde{B}=B_0\equiv B(q=1),\ k=C_{LDM},\ \widetilde{\kappa}=\kappa_0$ if $q\sim q_0$ and $\widetilde{B}=B_f\equiv B(q=q_f),\ k=-\widetilde{C}_{LDM},\ \widetilde{\kappa}=\kappa_f=\kappa_0/q_f^2$ if $q\sim q_f$. Differentiating Eq. (25) over time, we will look for the solution to Eq. (25) in the form

$$\Delta q=\sum_{i=1}^{3}C_i\exp(\lambda_i t). \tag{26}$$

Here the coefficients C_i are derived by the initial conditions. The eigenvalues λ_i are obtained as a solution to the following secular equation

$$(\lambda^2+\frac{k}{\widetilde{B}})(\lambda+\frac{1}{\tau})+\frac{\widetilde{\kappa}}{\widetilde{B}}\lambda=0. \tag{27}$$

In the case of the zero relaxation time limit, $\tau\to 0$, one obtains from Eq. (27) a non-damped motion with $\lambda=\pm\sqrt{k/\widetilde{B}}$, i.e., the time evolution is derived by the LDM stiffness coefficients C_{LDM} or $\widetilde{C}_{LDM}$. In the opposite case of rare collisions, $\tau\to\infty$, the solution to Eq. (27) leads to a non-damped motion with $\lambda=\pm\sqrt{(k+\widetilde{\kappa})/\widetilde{B}}$. In contrast to the previous case, the additional contribution, $\widetilde{\kappa}$, appears at the stiffness coefficient $k+\widetilde{\kappa}$ because of the Fermi surface distortion effect. In the case of the nuclear Fermi liquid one has $\widetilde{\kappa}\gg|k|$ [4,5]. This fact is important for the description of the nuclear isoscalar giant resonances [4,5]. Considering a motion near the ground state at $q\sim q_0=1$ with $k=C_{LDM}$, one obtains from Eq. (27) the quadrupole eigenvibrations with the eigenenergy

$$\hbar\omega_{2^+}=\hbar\sqrt{\frac{C_{LDM}+\kappa_0}{B_0}}\approx\hbar\sqrt{\frac{4\epsilon_F}{mR_0^2}}\approx 64.5\ A^{-1/3}\ \text{MeV}, \tag{28}$$

where $\epsilon_F=(9\pi)^{2/3}\hbar^2/8mr_0^2=34.73$ MeV is the Fermi energy and we adopt $r_0=1.18$ fm. The result (28) coincides with the analogous one obtained earlier by Nix and Sierk [4] and agrees with the experimental value of the energy of the isoscalar quadrupole resonance $\hbar\omega_{2^+}^{\rm exp}\approx 63\cdot A^{-1/3}$ MeV.

As can be seen from Eq. (27), the motion is damped for the non-zero and finite relaxation time τ. In the case of small amplitude motion near the ground state, $q\sim q_0$, the solution to

Eq. (25) at $t - t_0 \gg \tau$ takes the form of eigenvibrations with $\Delta q(t) \sim \exp(i\omega t)$, where the eigenfrequency ω is derived by [5]

$$\omega^2 B_0 = C_{LDM} + C'(\omega) - i\omega\gamma(\omega), \tag{29}$$

where $B_0 = B(q = 1)$, the additional stiffness coefficient, $C'(\omega)$, appears due to the Fermi surface distortion effect

$$C'(\omega) = \kappa_0 \, \mathrm{Im}\left(\frac{\omega\tau}{1 - i\omega\tau}\right) \tag{30}$$

and the friction coefficient $\gamma(\omega)$ is given by

$$\gamma(\omega) = \kappa_0 \, \mathrm{Re}\left(\frac{\tau}{1 - i\omega\tau}\right) = (4/m) \; \pi \; R_0^3 \; \eta_0 \, \mathrm{Re}\left(\frac{1}{1 - i\omega\tau}\right). \tag{31}$$

Here, $\eta_0 = (1/5) \; \rho_0 \; p_F^2 \; \tau$, is the classical viscosity coefficient [3].

Let us consider now the small amplitude motion (starting path for the development of the instability) near the saddle point, $q \sim q_f$, at finite relaxation time. We have evaluated numerically the value of Δq from Eq. (23) using the secular equation (27) and the initial conditions $\Delta q(t_0) = 0$, $\Delta \dot{q}\,(t_0) = v_0$ and $\Delta \ddot{q}\,(t_0) = 0$. In Fig. 2 we show the result for two values of the relaxation time $\tau = 3 \cdot 10^{-23}$s and $\tau = 4 \cdot 10^{-22}$s. We have used the following parameters $q_f = 1.6$, $A = 236$ and $\hbar\omega_f = \hbar\sqrt{|\widetilde{C}_{LDM}|/B_f} = 1.16$ MeV. The initial velocity v_0 was derived using the initial kinetic energy $E_{\mathrm{kin},0} = (1/2)B_f v_0^2 = 1$ MeV. In the case of the very short relaxation time, $\tau = 3 \cdot 10^{-23}$s, the memory effects in Eq. (25) play a minor role only and the amplitude of motion is approximately an exponentially growing function, similar to the case of Newton motion from the barrier in the presence of the friction forces, see curve 1 in Fig. 2. The friction coefficient γ can be derived here from Eq. (25) at $\omega_{F,f} \; \tau \ll 1$ and it is given by $\gamma = \gamma_f = \kappa_f \; \tau = \omega_{F,f}^2 \; B_f \; \tau \sim \tau$, where $\omega_{F,f} = \sqrt{\kappa_f / B_f}$ is the characteristic frequency for the eigenvibrations caused by the Fermi surface distortion effect. The behavior of $\Delta q(t)$ is changed dramatically with an increase of the relaxation time. At large enough relaxation time, the descent from the barrier is accompanied by the damped oscillations (curve 2 in Fig. 2). These oscillations are due to the memory integral in Eq. (25). The characteristic frequency, ω_R, and the corresponding damping parameter, ω_I, can be derived from the imaginary and real parts of complex conjugated roots of Eq. (27) as $\lambda = -\omega_I \pm i \; \omega_R$. The solution (26) takes then the form

$$\Delta q = C_\zeta \; e^{\zeta t} + A_\omega e^{-\Gamma t/2\hbar} \sin(Et/\hbar) + B_\omega e^{-\Gamma t/2\hbar} \cos(Et/\hbar), \tag{32}$$

where $\Gamma = 2\omega_I\hbar$ and $E = \omega_R\hbar$. In Fig. 3 we show the dependence of the instability growth rate parameter ζ, the energy of eigenvibrations E and the damping parameter Γ on the relaxation time τ.

In the rare collision regime $\omega_{F,f} \; \tau \gg 1$, the friction coefficient γ is obtained from Eq. (25) as $\gamma = \gamma_f = B_f \; /\tau \sim 1/\tau$. We point out that the τ-dependence of the friction coefficient, $\gamma_f \sim 1/\tau$, in the rare collision regime is opposite to the τ-dependence of $\gamma_f \sim \tau$ in the frequent collision regime. This is a consequence of the memory effects in the Fermi liquid. Below we will use the following extrapolation form for the friction coefficient near the fission barrier

$$\gamma_f = \omega_{F,f}\ B_f\ \frac{\omega_{F,f}\ \tau}{1+(\omega_{F,f}\ \tau)^2}. \tag{33}$$

The presence of the memory effects in the equation of motion (25) changes significantly the trajectory of the nuclear descent from the fission barrier. The result of the solution of Eq. (25) for the trajectory $\dot{q}\ (q)$ for the large amplitude motion from the saddle point q_f is shown in Fig. 4 (solid line). The dashed line in Fig. 4 shows the trajectory obtained as a solution to the Newton's equation (no memory effect)

$$B(q)\ \ddot{q} + \frac{\partial B(q)}{\partial q}\ \dot{q}^{\,2} = -\ \frac{\partial E_{\rm pot}(q)}{\partial q} - \gamma_f\ \dot{q}, \tag{34}$$

where the friction coefficient γ_f was taken from Eq. (33). In both cases we have used the initial conditions with $q(t_0) = q_f$, $\dot{q}\ (t_0) = \sqrt{2E_{\rm kin,0}/B_f}$ and $E_{\rm kin,0} = 1$ MeV and the relaxation time $\tau = 4 \cdot 10^{-22}$s. As seen from Fig. 4, the memory effect leads to the drift of q in time which is accompanied by the time oscillations of q along the trajectory of descent to the "scission" point, $q_{\rm sc}$. In Fig. 4, the time oscillations of q appear as a spiral-like behavior of the trajectory $\dot{q}\ (q)$. In both cases, the drift from the barrier is caused by the conservative force $-\ \partial E_{\rm pot}(q)/\partial q$. The oscillations appear due to the presence of the time-reversible elastic force in the memory integral in Eq. (25), see also Fig. 2. We point out that the memory integral contains the time-irreversible part also. Due to this fact, the velocity of the system decreases and the trajectory is shifted to the slope of the fission barrier. This effect is significantly stronger in the presence of the memory effects and leads to an essential delay of the descent process with respect to the analogous result obtained from the Newton's motion of Eq. (34). The influence of the memory effect on the descent time $t_{\rm sc}$ from the barrier to the "scission" point $q_{\rm sc}$ is shown in Fig. 5. As seen from Fig. 5, in the absence of the memory effects (dashed lines), the descent time $t_{\rm sc}$ is about $1 \div 3 \cdot 10^{-21}$s and, as it should be, the value of $t_{\rm sc}$ goes to the limit of non-friction motion for both the frequent collision regime, $\tau \to 0$, and the rare collision regime, $\tau \to \infty$. This property of the descent with no-memory effects is the result of the Fermi-liquid approximation (33) for the friction coefficient γ_f in Eq. (34). In contrast to this case, the descent time $t_{\rm sc}$ evaluated in the presence of the memory effects (solid lines) grows monotonously with the relaxation time τ. The additional delay of the motion in the rare collision region (large τ) is here caused by the contribution of the elastic force due to the memory integral. The elastic force leads to the dynamical renormalization of the adiabatic force $-\ \partial E_{\rm pot}(q)/\partial q$ in Eq. (23) and acts against the force $-\ \partial E_{\rm pot}(q)/\partial q$.

Let us apply our approach to the case of symmetric nuclear fission described by Eq. (15), assuming the Lorentz parameterization for the profile function $Y(z)$ in Eq. (12) in the following form [1],

$$Y^2(z) = (z^2 - \zeta_0^2)(z^2 + \zeta_2^2)/Q\,, \tag{35}$$

where the multiplier Q guarantees the volume conservation,

$$Q = -[\zeta_0^3(\frac{1}{5}\zeta_0^2 + \zeta_2^2)]/R_0^3\,. \tag{36}$$

Here all quantities of the length dimension are expressed in the R_0 units. The parameter ζ_0 in (35) determines the general elongation of the figure and ζ_2 is related to the radius of the neck. For $\zeta_2 = \infty$ the shapes (35) coincide with the spheroidal ones. At finite ζ_2 ($\zeta_2 > 0$ for bound figures) the neck appears and the value $\zeta_2 = 0$ corresponds to the scission point after which the figure is divided in the two parts for $\zeta_2 < 0$. To solve Eq. (15) we will rewrite it as a set of two equations. Namely,

$$\sum_{j=1}^{2}[B_{ij}(q)\ddot{q}_j + \sum_{k=1}^{2}\frac{\partial B_{ij}}{\partial q_k}\ \dot{q}_j\dot{q}_k] = -\frac{\partial E_{\rm pot}(q)}{\partial q_i} + R_i(t,q) \tag{37}$$

and

$$\frac{\partial R_i(t,q)}{\partial t} = -\frac{R_i(t,q)}{\tau} + \sum_{j=1}^{2}\kappa_{ij}(q,q)\dot{q}_j \qquad \text{at} \qquad R_i(t=0,q) = 0, \tag{38}$$

where $q = \{q_1, q_2\} = \{\zeta_0, \zeta_2\}$ and the terms $\sim \dot{q}_i\dot{q}_j$ were omitted in Eq. (38), as the next order corrections. The kernel $\kappa_{ij}(q,q)$ is given by

$$\kappa_{ij}(q,q) = \frac{2}{5}m\rho_0 v_F^2 \int d\mathbf{r}\ (\nabla_\nu\nabla_\mu\ \bar{\phi}_i\ (\mathbf{r},q))\ (\nabla_\nu\nabla_\mu\ \bar{\phi}_j\ (\mathbf{r},q)). \tag{39}$$

We have performed numerical calculation for symmetric fission of the nucleus ^{236}U. We solved Eqs. (37) and (38) numerically using the deformation energy $E_{\rm pot}(q)$ from Refs. [1,28]. The scission line was derived from the condition of the instability of the nuclear shape with respect to the variations of the neck radius:

$$\frac{\partial^2 E_{\rm pot}(q)}{\partial \rho_{\rm neck}^2} = 0 \tag{40}$$

where $\rho_{\rm neck} = \zeta_2/\sqrt{\zeta_0(\zeta_0^2/5 + \zeta_2^2)}$ is the neck radius. The equations of motion (37) and (38) were solved with the initial conditions corresponding to the saddle point deformation and the initial kinetic energy $E_{\rm kin,0} = 1$ MeV (initial neck velocity $\dot{\zeta}_2 = 0$). To solve the Neumann problem (14) for the velocity field potential we have used the method based on the theory of the potential, see Ref. [25].

In Fig. 6 we show the dependence of the fission trajectory, i.e., the dependence of the neck parameter ζ_2 on the elongation ζ_0, for the fissioning nucleus ^{236}U for two different values of the relaxation time τ: $\tau = 4\cdot 10^{-22}$s (dashed line) and $\tau = 0$ (dotted line). The scission line (dot-dashed line in Fig. 6) was obtained as a solution to Eq. (40). We define the scission point as the intersection point of the fission trajectory with the scission line. As can be seen from Fig. 6 the memory effect hinders slightly the neck formation and leads to a more elongated scission configuration. To illustrate the memory effect on the observable values we have evaluated the translation kinetic energy of the fission fragments at infinity, $E_{\rm kin}$, and the prescission Coulomb interaction energy, $E_{\rm Coul}$. The value of $E_{\rm kin}$ is the sum of the Coulomb interaction energy at scission point, $E_{\rm Coul}$, and the prescission kinetic energy $E_{\rm kin,ps}$. Namely,

$$E_{\rm kin} = E_{\rm Coul} + E_{\rm kin,ps}. \tag{41}$$

After scission the fission fragments were described in terms of two equal mass spheroids (see Ref. [17]). We assumed that the distance between the centers of mass, d, of two spheroids is equal to the distance between the two halves of the fissioning nucleus at the scission point:

$$d = \frac{5}{4}\zeta_0 \frac{\zeta_0^2 + 3\zeta_2^2}{\zeta_0^2 + 5\zeta_2^2}|_{\rm scis} \ . \tag{42}$$

The corresponding velocity $\dot{d}$ was obtained by the differentiation of Eq. (42) with respect to the time. The elongation, c, of both separated spheroids is defined by the condition:

$$2c + d = 2\zeta_{0,\rm scis} \tag{43}$$

where $\zeta_{0,\rm scis}$ is the elongation of the nucleus at the scission point. The collective parameters c and d and the velocity $\dot{d}$ were then used to evaluate the Coulomb energy $E_{\rm Coul}$ (see Ref. [1]) and the prescission kinetic energy $E_{\rm kin,ps}$ in Eq. (41).

The influence of the memory effects on the fission-fragment kinetic energy, $E_{\rm kin}$, and the prescission Coulomb interaction energy, $E_{\rm Coul}$, is shown in Fig. 7. As seen from Fig. 7 the memory effects are neglected at the short relaxation time regime where the memory integral is transformed into the usual friction force. In the case of the Markovian motion with friction (dashed line), the yield of the potential energy, $\Delta E_{\rm pot}$, at the scission point is transformed into both the prescission kinetic energy, $E_{\rm kin,ps}$, and the time irreversible dissipation energy, $E_{\rm dis}$, providing $\Delta E_{\rm pot} = E_{\rm kin,ps} + E_{\rm dis}$. In contrast to this case, the non-Markovian motion with the memory effects (solid line) produces an additional time reversible prescission energy, $E_{\rm F,ps}$, caused by the distortion of the Fermi surface. In this case, the energy balance reads $\Delta E_{\rm pot} = E_{\rm kin,ps} + E_{\rm dis} + E_{\rm F,ps}$. We point out that the two-spheroid parametrization of the fissioning nucleus at the scission point given by Eqs. (42) and (43), used in this work, leads to the prescission Coulomb energy $E_{\rm Coul}$ which is about 5 MeV lower (for ^{236}U) than the Coulomb interaction energy of the scission point shape [18]. Taking into account this fact and using the experimental value of the fission-fragment kinetic energy $E_{\rm kin}^{\rm exp} = 168$ MeV [18], one can see from Fig. 7 that the Markovian motion with friction (dashed line) leads to the overestimate of the fission-fragment kinetic energy $E_{\rm kin}$. In the case of the non-Markovian motion with the memory effects (solid line), a good agreement with the experimental data is obtained at the relaxation time of about $\tau = 8 \cdot 10^{-23}$s. A small deviation of the prescission Coulomb energy $E_{\rm Coul}$ obtained at the non-Markovian motion (solid line in Fig. 7) from the one at the Markovian motion (dashed line in Fig. 7) is caused by the corresponding deviation of both fission trajectories in Fig. 6.

In Fig. 8 we illustrate the memory effect on the saddle-to-scission time $t_{\rm sc}$. In the case of the non-Markovian motion (solid line), the delay in the descent of the nucleus from the barrier grows with the relaxation time τ (at $\tau \geq 4 \cdot 10^{-23}$s). This is mainly due to the hindering action of the elastic force caused by the memory integral. The saddle-to-scission time increases by a factor of about 2 due to the memory effect at the "experimental" value of the relaxation time $\tau = 8 \cdot 10^{-23}$s which was derived from the fit of the fission-fragment kinetic energy $E_{\rm kin}$ to the experimental value of $E_{\rm kin}^{\rm exp}$ (see above).

IV. SUMMARY AND CONCLUSIONS

By use of **p**-moments techniques, we have reduced the collisional kinetic equation to the equations of motion for the local values of particle density, velocity field and pressure tensor. The obtained equations are closed due to the restriction on the multipolarity l of the Fermi surface distortion up to $l = 2$. To apply our approach to the nuclear large amplitude motion, we have assumed that the nuclear liquid is incompressible and irrotational. We have derived the velocity field potential, $\phi(\mathbf{r},q)$, which depends then on the nuclear shape parameters $q(t)$ due to the boundary condition on the moving nuclear surface. Finally, we have reduced the problem to a macroscopic equation of motion for the shape parameters $q(t)$. Thus we consider a change (not necessary small) of the nuclear shape which is accompanied by a small quadrupole distortion of the Fermi surface. The obtained equations of motion for the collective variables $q(t)$ contains the memory integral which is caused by the Fermi-surface distortion and depends on the relaxation time τ.

The memory effects on the nuclear collective motion disappear in two limits; of zero relaxation time, $\tau \to 0$, and at $\tau \to \infty$. In general case, the memory integral contains the contribution from both the time reversible elastic force and the dissipative friction force. The eigenmotion near the ground state (point A in Fig. 1) is influenced by memory effects through the frequency dependency of the stiffness, $C'(\omega)$, and the friction, $\gamma(\omega)$, coefficients in the dispersion equation (29). We point out that the friction coefficient $\gamma(\omega)$ in our approach (see Eq. (31)) changes its τ-dependency from $\gamma \sim \tau$ in the frequent collision regime, $\omega_R\tau \ll 1$, to $\gamma \sim 1/\tau$ in the rare collision regime, $\omega_R\tau \gg 1$. Due to this fact, we have obtained a correct description of the zero-to-first sound transition in the nuclear Fermi-liquid [5]. In the limit of $\tau \to \infty$, the additional contribution (elastic force) in Eq. (25) appears due to the memory integral. The contribution from the elastic force is significantly stronger than the one caused by the adiabatic force $-\,k\,\Delta q$. The presence of the elastic force provides a correct A-dependence of the energy of the isoscalar giant multipole resonances.

We have shown that the development of instability near the fission barrier (point B in Fig. 1) is strongly influenced by the memory effects if the relaxation time τ is large enough. In this case, a drift of the nucleus from the barrier to the scission point is accompanied by characteristic shape oscillations (see Figs. 2 and 3) which depend on the parameter $\widetilde{\kappa}$ of the memory kernel and on the relaxation time τ. The shape oscillations appear due to the elastic force induced by the memory integral. The elastic force acts against the adiabatic force $-\,\partial E_{\rm pot}(q)/\partial q$ and hinders the motion to the scission point C. In contrast to the case of the Markovian motion, the delay in the fission is caused here by the conservative elastic force and not only by the friction force. Due to this fact, the nucleus loses a part of the prescission kinetic energy converting it into the potential energy of the Fermi surface distortion instead of the time-irreversible heating of the nucleus. As mentioned above, in the nuclear Fermi liquid the friction coefficient γ is a non-monotonic function of the relaxation time τ (see Eqs. (31) and (33)) providing the asymptotic behavior $\gamma \sim \tau$ and $\gamma \sim 1/\tau$ in both limiting cases of the frequent and rare collisions, respectively. This feature of γ leads to the non-monotonic behavior of the saddle-to-scission time, $t_{\rm sc}$, as function of τ in the case of the Markovian (no memory) motion with friction, see dashed lines in Figs. 5 and 8. In contrast to the Markovian motion, the memory effects provide a monotonous dependence of the saddle-to-scission time on the relaxation time τ (see solid lines in Figs. 5 and 8). This is

caused by the elastic forces produced by the memory integral, which lead to the additional hindrance for the descent from the barrier at large τ.

The memory effects lead to the decrease of the fission-fragment kinetic energy, $E_{\rm kin}$, with respect to the one obtained from the Markovian motion with friction, see Fig. 7. This is because a significant part of the potential energy at the scission point is collected as the energy of the Fermi surface deformation. Note that the decrease of the fission-fragment kinetic energy due to the memory effects is enhanced in the rare collision regime (at larger relaxation time) while the effect due to friction decreases. An additional source for the decrease of the fission-fragment kinetic energy is caused by the shift of the scission configuration to that with a larger elongation parameter ζ_0, in the case of the non-Markovian motion, see Fig. 6. Due to this fact, the repulsive Coulomb energy of the fission fragments at the scission point decreases with respect to the case of the Markovian motion.

ACKNOWLEDGMENTS

This work was supported in part by the US Department of Energy under grant # DOE-FG03-93ER40773. We are grateful for this financial support. One of us (V.M.K.) thanks the Cyclotron Institute at Texas A&M University for the kind hospitality.

REFERENCES

[1] R. W. Hasse and W. D. Myers, *Geometrical Relationships of Macroscopic Nuclear Physics* (Springer-Verlag, Berlin, 1988).
[2] M. Brack et al., Rev. Mod. Phys., **44**, 320 (1972).
[3] A. A. Abrikosov and I. M. Khalatnikov, Rep. Progr. Phys. **22**, 329 (1959).
[4] J. R. Nix and A. J. Sierk, Phys. Rev. C **21**, 396 (1980).
[5] D. Kiderlen, V. M. Kolomietz and S. Shlomo, Nucl. Phys. **A608**, 32 (1996).
[6] E. M. Lifshitz and L. P. Pitaevsky, *Physical kinetics*, (Pergamon Press, Oxford - New York - Seoul - Tokyo, 1993).
[7] C. J. Pethick and D. G. Ravenhall, Ann. of Phys. **183**, 131 (1988).
[8] D. Vautherin and D. M. Brink, Phys. Rev. C **5,** 626 (1973).
[9] A. Kolomiets, V. M. Kolomietz and S. Shlomo, Phys. Rev. C **59,** 3139 (1999).
[10] H. Grabert, P. Schramm and G. -L. Ingold, Phys. Rep. **168**, 115 (1988).
[11] Y. Abe, S. Ayik, P. -G. Reinhard and E. Suraud, Phys. Rep. **275**, 49 (1996).
[12] S. Ayik and D. Boilley, Phys. Lett. **B276**, 263 (1992); **B284**, 482(E) (1992).
[13] V. M. Kolomietz, A. G. Magner and V. A. Plujko, Nucl. Phys. **A545**, 99c (1992).
[14] S. Ayik, E. Suraud, J. Stryjewski and M. Belkacem, Z. Phys. **A337**, 413 (1990).
[15] D. Boilley, Y. Abe, S. Ayik and E. Suraud, Z. Phys. **A349**, 119 (1994).
[16] D. Boilley, E. Suraud, Y. Abe and S. Ayik, Nucl. Phys. **A556**, 67 (1993).
[17] J. R. Nix and W. J. Swiatecki, Nucl. Phys. **71**, 1 (1965).
[18] K. T. R. Davies, R. A. Managan, J. R. Nix and A. J. Sierk, Phys. Rev. C **16**, 1890 (1977).
[19] J. Schirmer, S. Knaak and G. Süssmann, Nucl. Phys. **A199**, 31 (1973).
[20] V. M. Kolomietz and H. H. K. Tang, Phys. Scripta **24**, 915 (1981).
[21] G. Holzwarth and G. Eckart, Nucl. Phys. **A325**, 1 (1979).
[22] V. M. Kolomietz, *Local density approach for atomic and nuclear physics* (Naukova dumka, Kiev, 1990) (in Russian).
[23] V. M. Kolomietz, Sov. J. Nucl. Phys. **37**, 325 (1983).
[24] K. T. R. Davies, A. J. Sierk and J. R. Nix, Phys. Rev. C **13**, 2385 (1976).
[25] F. A. Ivanyuk, V. M. Kolomietz and A. G. Magner, Phys. Rev. C **52**, 678 (1995).
[26] H. A. Kramers, Physica **7**, 284 (1940).
[27] J. R. Nix, A. J. Sierk, H. Hofmann et al., Nucl. Phys. **A424**, 239 (1984).
[28] W. D. Myers and W. J. Swiatecki, Ark. Fys. **36**, 343 (1967).
[29] D. Vautherin, Phys. Lett. **57B**, 425 (1975).
[30] L. D. Landau and E. M. Lifshitz, *Fluid Mechanics* (Pergamon Press, Oxford, 1959).
[31] V. L. Berdichevsky, *Variational Principle for Mechanics of Continua* (Nauka, Moscow, 1983) (in Russian).
[32] L. D. Landau and E. M. Lifshitz, *Statistical physics* (Pergamon Press, Oxford, 1958).

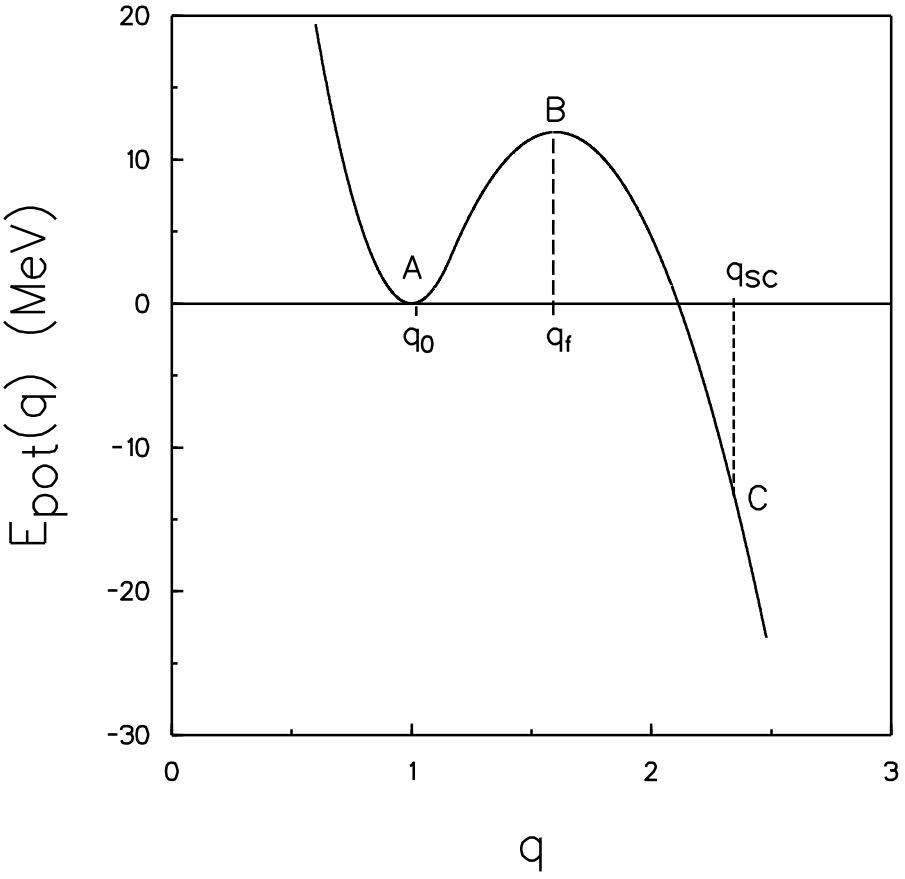

Fig. 1

FIG. 1. Dependence of the potential energy $E_{\rm pot}$ on the shape parameter q.

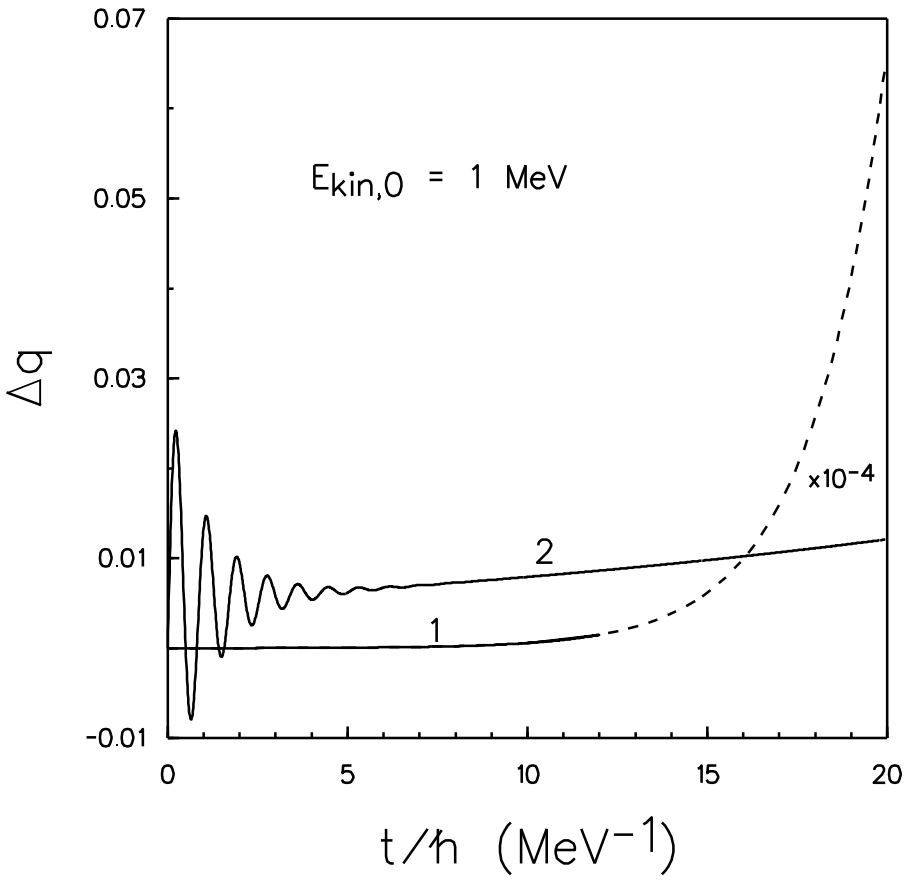

FIG. 2. Time variation of the shape parameter q near the saddle point B (see Fig. 1), for varios values of the relaxation time τ. The curves 1 and 2 correspond to the values of $\tau = 3 \cdot 10^{-23}$s $\tau = 4 \cdot 10^{-22}$s, respectively.

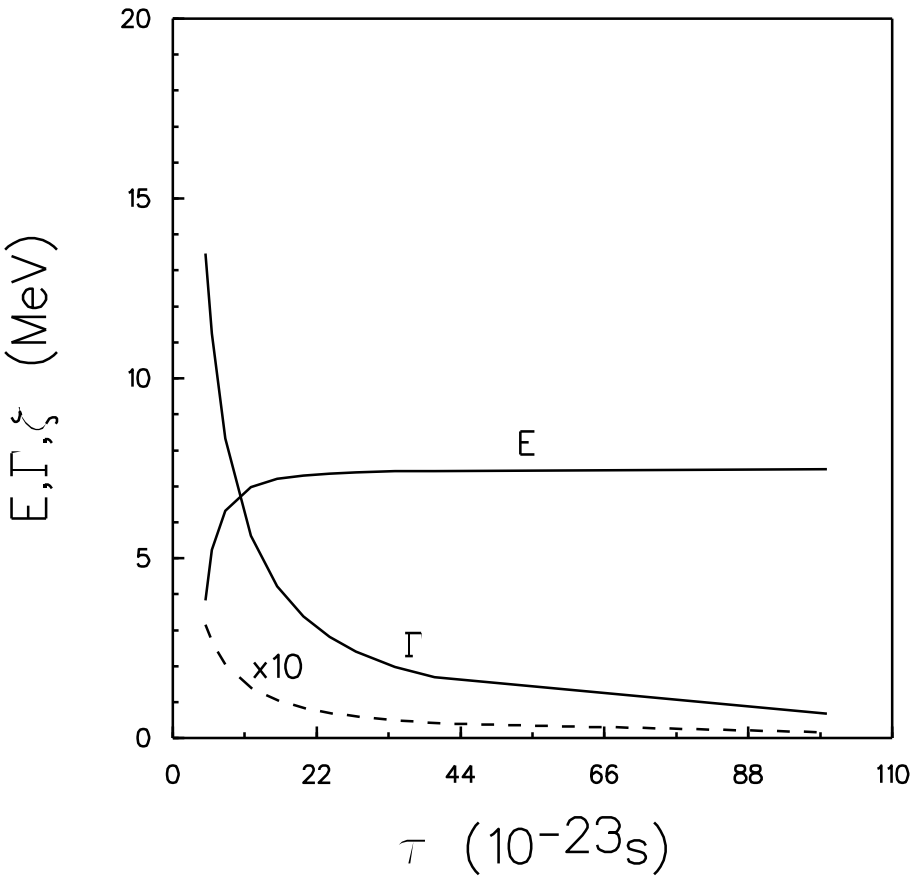

FIG. 3. Dependence upon relaxation time τ of the characteristic energy E and width Γ of oscillations (solid lines) and the instability growth rate parameter ζ (dashed line) for the curve 2 in Fig. 2.

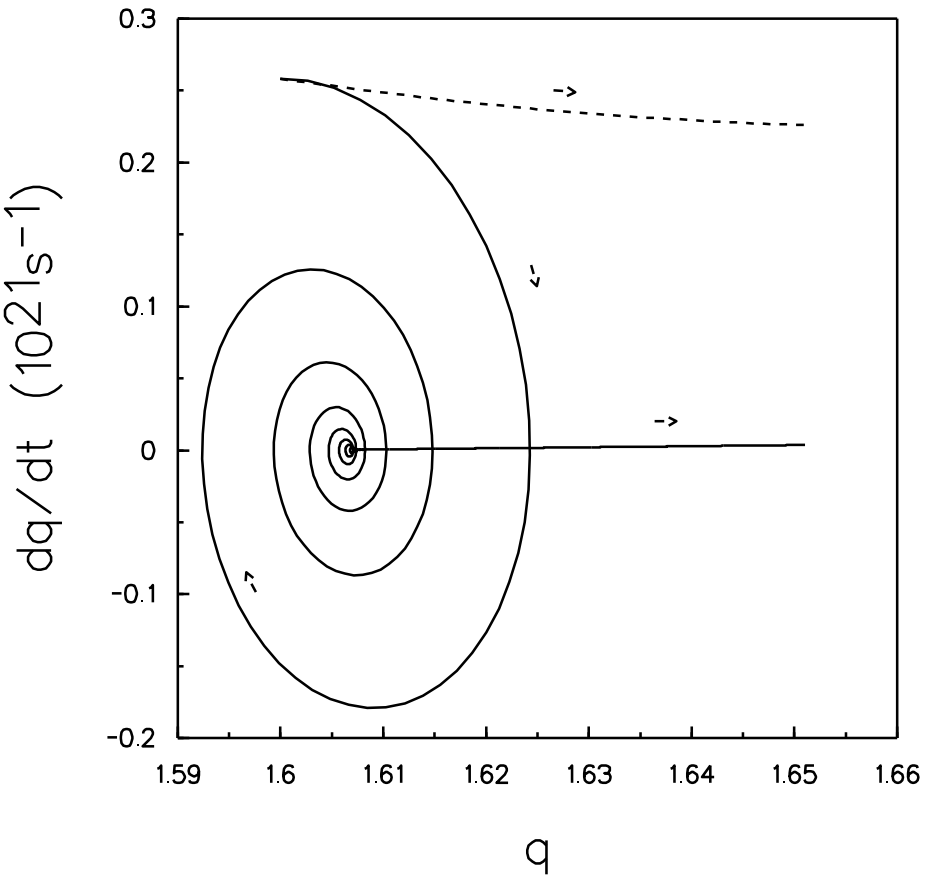

FIG. 4. Trajectory (dependence of the collective velocity dq/dt on the collective coordinate q) for the descent from the saddle point B (see Fig. 1). Solid line represents the result of the calculation in presence of the memory effects and dashed line is for the case of Markovian (no memory) motion with the friction forces. We have used the relaxation time $\tau = 4 \cdot 10^{-22}$s and the initial kinetic energy $E_{\rm kin} = 1\,{\rm MeV}$.

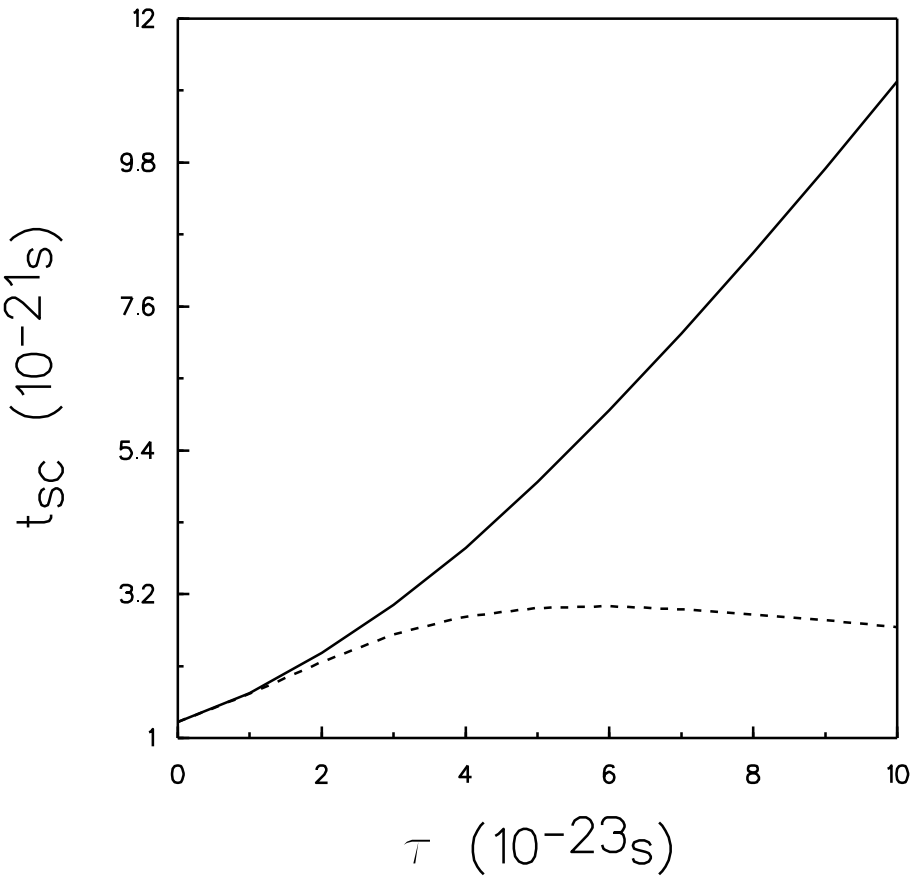

FIG. 5. Dependence upon relaxation time τ of the time, $t_{\rm sc}$, required to travel a nucleus from the saddle point B to the "scission" point C (see Fig. 1). Solid line represents the result of the calculation in presence of the memory effects and dashed line is for the case of Markovian (no memory) motion with the friction forces. The initial kinetic energy is $E_{\rm kin} = 1\,{\rm MeV}$.

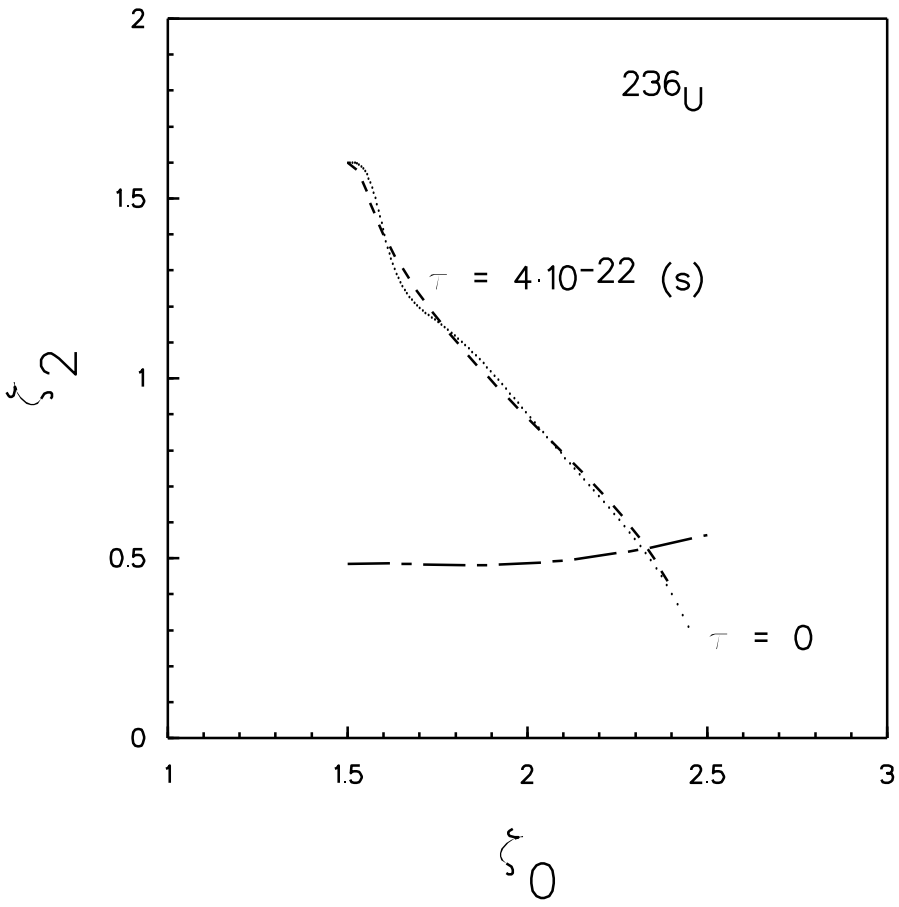

FIG. 6. Trajectories of descent from the saddle point of the nucleus ^{236}U in the ζ_0, ζ_2 plane. Dashed line represents the result of the calculation in presence of the memory effects and dotted line is for the case of Markovian (no memory) motion with the friction forces. We have used the relaxation time $\tau = 4 \cdot 10^{-22}$s and the initial kinetic energy $E_{\rm kin} = 1\,$MeV. Dot-dashed line is the scission line derived from the condition (43).

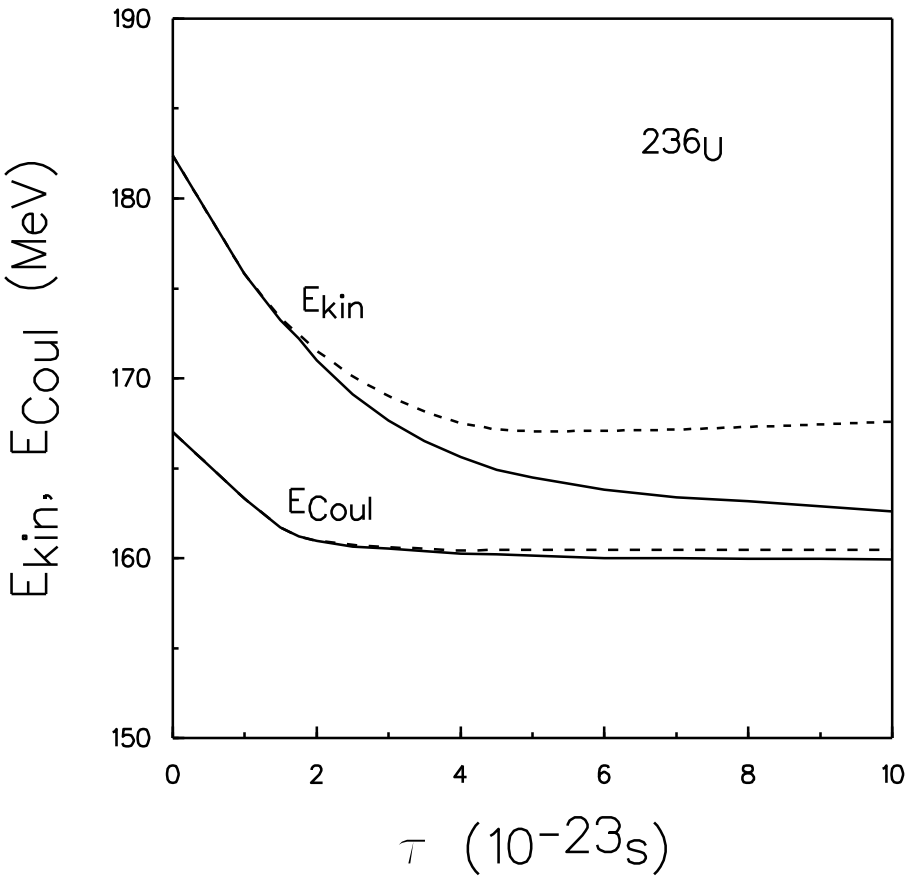

FIG. 7. Fission-fragment kinetic energy, $E_{\rm kin}$, (curves 1) and the Coulomb repulsive energy at the scission point, $E_{\rm Coul}$, (curves 2) versus the relaxation time τ for the nucleus ^{236}U. Solid lines represent the result of the calculation in presence of the memory effects and dashed lines are for the case of Markovian (no memory) motion with the friction forces. The initial kinetic energy is $E_{\rm kin,0} = 1\,{\rm MeV}$.

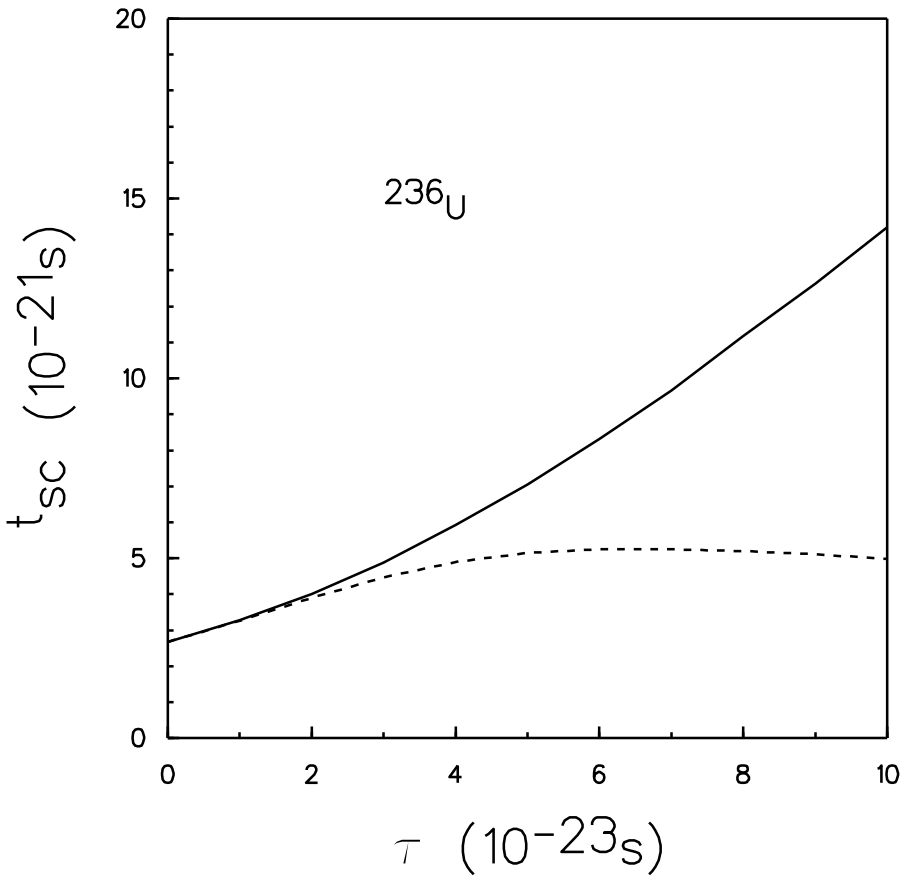

FIG. 8. Dependence upon relaxation time τ of the saddle-to-fission time, $t_{\rm sc}$, for the descent from the barrier in the case of two-dimension (ζ_0, ζ_2) parametrization for the nucleus ^{236}U. Solid line represents the result of the calculation in presence of the memory effects and dashed line is for the case of Markovian (no memory) motion with the friction forces. The initial kinetic energy is $E_{\rm kin} = 1\,{\rm MeV}$.